International Journal of Natural and Engineering Sciences 8 (2): 47-56, 2014
ISSN: 1307-1149, E-ISSN: 2146-0086, www.nobel.gen.tr

Transient Response of Cracks Emanated from a Circular Hole under Impact Loading

Mohammad DAMGHANI NOURI[1] Hossein RAHMANI[1*]
[1]Department of Mechanical Engineering, Semnan University, Semnan, Iran

*Corresponding author:
Email: hrme80@gmail.com

Received: July 16, 2014
Accepted: August 27, 2014

Abstract
The transient stress field around a finite crack emanated from a circular hole is obtained using integral transforms method. The normal and shear tractions applied to cracks surface. Firstly, the dynamic stress concentration factor around the circular hole without crack is calculated and secondly, the concentration stress around the hole is applied to the crack surface and the stress filed in the crack tip and dynamic stress intensity factor is obtained. Because of the normal and shear stress, the mode I and II of fracture happen. Finally, the results are compared with previous studies.

Keyword: Dynamic Stress Intensity Factor, Impact, Crack, Fracture

INTRODUCTION

In structures, due to the stress concentration around the holes, particularly, cracks will initiate and propagate from the hole.

Fracture behavior of materials under impact and dynamic loads is different from static mode. Inertia, reflection of stress waves, and the effects of the strain rate dependent behavior of material are among the differences between dynamic and static fracture behaviors. Consequently, problems for dynamic stress concentration factor around a hole got much attention by many investigators.

Pao studied The Stress concentrations around a circular cavity in an infinitely extended, thin elastic plate, during passage of plane compressional waves. In this research, the harmonic waves were applied to the circular hole and the dynamical stress concentration factors were found to be dependent on the incident wave length and Poisson's ratio for the plate.[1]

Diffraction of a Pressure Wave by a Cylindrical Cavity in Elastic medium was investigated analytically by Baron and Matthews. In this research, the stress concentration around a circular hole under plane shock wave whose front is parallel to the axis of the cavity, were calculated.[2]

In the similar paper, Baron and Matthews studied the displacement and velocities produced by the diffraction of a pressure wave by a cylindrical cavity in an elastic medium.[3]

The experimental method, method of boundary Integrals and Laplace transform, the stress concentration around the cavity in the strip and shell and Scattering of flexural wave in a thin plate with multiple circular holes are some of the important researches about dynamic stress concentration factor and wave diffraction.[4-10]

Sih was one of the researchers who conducted an analytical study on the dynamic stress intensity factors of cracks and presented most basic methods for stress fields around crack tip and dynamic fracture [11].

Frund studied semi-infinite crack on unbounded body. He also studied dynamic stress intensity factor on different fracture modes using step function. In this analysis, the equations, which were obtained using the dual Laplace transform, were simplified and solved using the Wiener-Hopf method [12].

Sih and Embely in one article and Stephen and Tsin-Hwei in another article discussed the behavior of crack analysis with a limited length on an unbounded body in a 2-D mode. Using the Laplace transform and then the Fourier sine and cosine transforms, they analyzed the wave equations and the fields created around a crack. The obtained dual integral equations were solved using the numerical methods and the value of dynamic stress intensity factor around the crack was determined [13-14].

The effect of stress concentration on stress intensity factor may happen in cracks that emanated from holes.

Li-qing and Bing-zheng studied the dynamic stress concentration factor for a single hole-edge slant crack in a finite plate by finite element method. Due to the direction of crack relative to stress wave moving path, the mode I and II happen. [15-16]

Meguid and Wang investigated theoretically the treatment of the dynamic interaction between a crack and an arbitrarily located circular hole near its tip under incident anti-plane shear wave. The method of integral transform technique has been used for solving the equations.[17]

The scattering and diffraction of SH-waves and dynamic stress intensity factor in the crack emanating from circular or elliptical holes have been studied by several researchers.[18-21]

Also, the effect of anti-plane and the mode III of fracture and dynamic stress intensity factor emanating from holes have been investigated for different kinds of material such as piezoelectric, electromagnetic and etc.[22-25]

As we can see, the large numbers of these researches have been done numerically and analytically.

In experimental investigation for determining the dynamic stress intensity factor in crakes, originating from

holes, or radial crack we can mention the studies of Malezhik et al.[26]. They studied the dynamic fracture of plates weakened by holes with edge cracks and subjected to impulsive loading is studied using the dynamic photo elastic method.

Most of the references discussed earlier are for the effect of SH-waves and Anti-plane waves on dynamic stress intensity factor on crakes emanated from holes. There is a lack of results for the effect of in-plane waves on Dynamic stress intensity factor for cracks emanated from holes.

The present paper is based on the results obtained in [2, 7-8, 13] and investigates the dynamic interaction between hole and crack. The main objective of this study is to evaluate stresses field distribution and dynamic stress intensity factor in a crack that is emanated from a hole in an elastic medium. The paper is organized as follows: The problem statement is given in Sect. 2. The basic equation and solution of them is discussed in Sect. 3, and the numerical procedure, a series of numerical results and their comparison with old studies and discussion is shown in Sect. 4, 5, while and conclusions are given in Sect. 6.

PROBLEM STATEMENT

To determine the dynamic stress intensity for a crack emanated from a hole, firstly we need to know the stress fields near the tip of the crack [27-29]. In this study, firstly the stress distribution around the circular hole is calculated by the method that is solved in [2] and [8]. In those researches the stress around a circular hole are calculated analytically. Because of the difference in coordinate systems considered in those papers, we assume a new coordinate system and the analytical equation and solution of references [2] and [8] are rewrote and resolved for this coordinate system by a MATLAB code. After calculating the stress distribution around the circle hole, the stress distribution in the x direction and in angle 270^{o} calculated and this stress applied to the crack plane.

Finally the dynamic stress intensity factor equation is obtained and solved for the crack.

Consider an infinite elastic medium which contain a cavity as shown in

Figure **1**. A traction shock wave in time t=0 in direction –x, lies on a circle of radius R and diffract. The direction of the stress is opposite of the direction of motion because the wave is tensile stress.

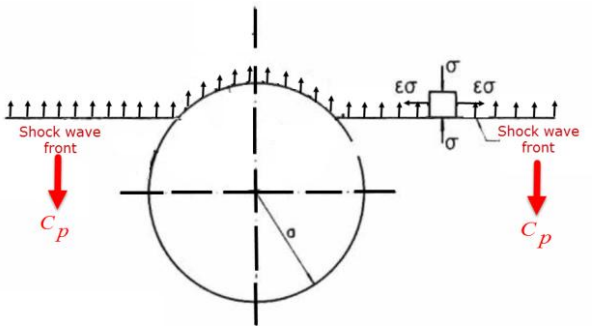

Figure 1. Shock wave propagation around the hole

When the first point of hole is acted on by the front of shock wave, the stress wave diffracts and a new distribution of stress forms around the hole. For calculating the new stress distributions around hole consider a coordinate system as shown in Figure **2**.

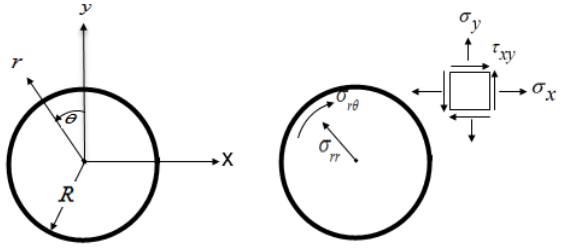

Figure 2. Coordinate system used for stress concentration analysis

The stress distribution around the circular hole was calculated in [2].

Based on [2], the hoop stress distribution around the hole is calculated from equations 1-4.

Due to the direction of a crack, we need to know the hoop stress only because the direction of the crack in later analysis is so that the radial and shear stresses are neglected.

$$\sigma_{\theta\theta}(t)=-\sigma_0\left[\sin^2\theta-\varepsilon\cos^2\theta\right]+\sigma_{\theta\theta 0}(t)+\sum_{n=1}^{\infty}\left[\tilde{\sigma}_{\theta\theta}(t)+\tilde{\tilde{\sigma}}_{\theta\theta}(t)\right]\cos n\theta \tag{1}$$

$$\frac{\sigma_{\theta\theta n}(r,\theta,t)}{\cos n\theta}=\frac{\sigma}{2\pi i}\int_{-\infty-i\gamma}^{\infty-i\gamma}\frac{I(r,\xi)e^{i\xi\frac{c_p t}{R}}}{\xi\left[FB+DE\right]}d\xi \tag{2}$$

$$F=\left[2n(n+1)-2\xi^2\right]H_m^{(2)}(\xi)-2\xi H_{n-1}^{(2)}(\xi)$$

$$B=\left[12n(n+1)+\frac{c_p^2}{c_s^2}\xi\right]H_m^{(2)}(\frac{c_p}{c_s}\xi)+2\frac{c_p}{c_s}\xi H_{n-1}^{(2)}(\frac{c_p}{c_s}\xi)$$

$$D=2n(n+1)H_m^{(2)}(\xi)-2n\xi H_{n-1}^{(2)}(\xi)$$

$$E=2n(n+1)H_m^{(2)}(\frac{c_p}{c_s}\xi)-2n\frac{c_p}{c_s}\xi H_{n-1}^{(2)}(\frac{c_p}{c_s}\xi)$$

$$I_n(r,\xi)=\left\{\left[B+kE\right]\left[2\xi\frac{R}{r}H_{n-1}^{(2)}(\xi\frac{r}{R})-\left\{(2n^2+2n)\frac{R^2}{r^2}+\xi^2\right\}H_n^{(2)}(\frac{r}{R}\xi)\right]+\left[kF-D\right]\left[2n(n+1)\frac{R^{(2)}}{r^2}H_n^2(\frac{c_p}{c_s}\xi\frac{r}{R})-2\frac{c_p}{rc_s}n\xi RH_{n-1}^{(2)}(\frac{c_p r}{c_s R}\xi)\right]\right\} \tag{3}$$

$$\frac{\sigma_{\theta\theta n}(r,t)}{c\sigma}=\int_{-\infty-i\gamma}^{\infty-i\gamma}\left[\frac{2\frac{a}{t}H_1^{(2)}(\frac{\zeta r}{a})+\zeta H_0^{(2)}(\frac{\zeta r}{a})}{\xi\left[3\zeta H_0^{(2)}(\zeta)-2H_1^{(2)}(\zeta)\right]}\right]e^{i\xi\frac{c_p t}{R}}d\xi \tag{4}$$

After $t=R/C_p$, the radial crack is affected by the front of shock wave.

In these equations, c_p is the velocity of plane stress, R is the radius of circular hole, ξ is a complex variable and $H^{(2)}$ is the hankel function(Bessel function of third kind).

These equations are solved by a MATLAB code and the hoop stress distribution around the circular hole is calculated. For this analysis, we assume that a tensile stress wave with magnitude σ_0 applied to the infinite 2D plate with a circular hole.

Figure **3** and Figure 4 shows the hoop stress distribution around the circular hole.

To validate the results for the stress concentration that is obtained in this research, 4 point is selected in around the circle as showed in Figure 5.

The history of stress in the a_1, a_2, a_3 and a_4 is showed in

Figure **6**. As it can be seen, the value of $\sigma_{\theta\theta}/\sigma_0$ in the circular boundary(r=R) is compared from [2] and the MATLAB code from this research(the yellow dashed curve and the solid black curve). Because of the direction of stress wave (pressure wave and tensile wave) these curves are similar in value and opposite in the direction.

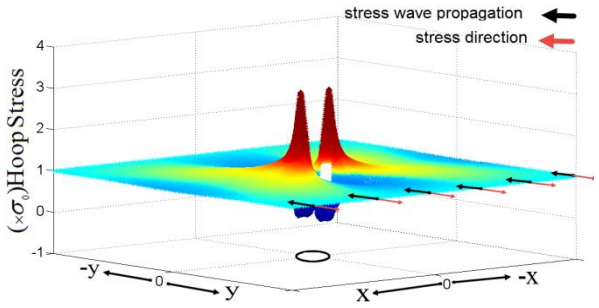

Figure 3. Hoop stress distribution in time 3.2 Ct/a around the hole in 3D view

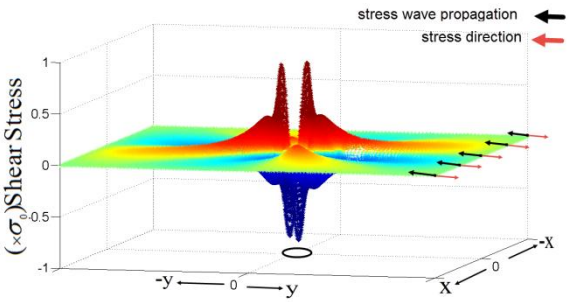

Figure 4. Hoop stress distribution around the circular hole in 2D view

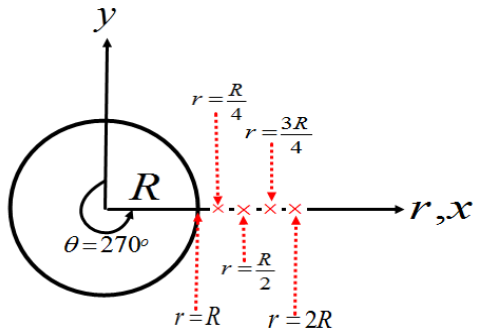

Figure 5. Selected points for calculating the hoop stress

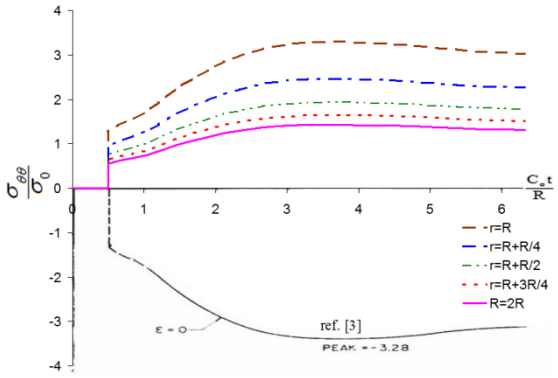

Figure 6. Hoop stress around the hole

In the

Figure **7** the stress changes via distance from the circle boundary in $\theta=270^o$ is showed in the time 3 Ct/20 that have the maximum value.

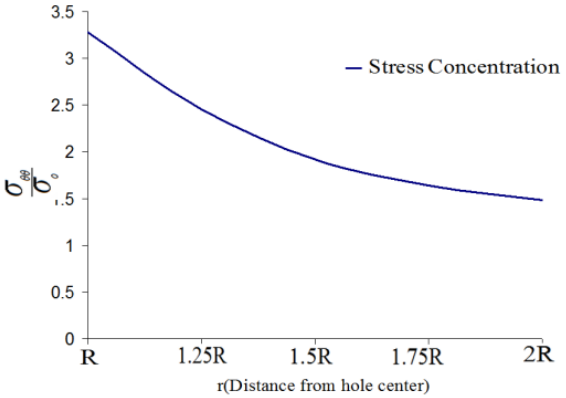

Figure 7. Stress distribution in x direction

As mentioned later, the purpose of this research is to calculate the DSIF in a crack that is emanated from a hole in radial direction and in $\theta=270^o$. so that the crack is exactly perpendicular to the stress wave propagation direction. Due to the direction of crack, it is needed to know the relation between stress, time and location in the crack path. For this reason, stress distribution is calculated for the line in x direction with the length of R as shown in

Figure **8**. the amount of radial and shear stresses are negligible in compared with hoop stress and so only the mode I of fracture occurs and the shear stress wave distribution and other modes of fracture is neglected.

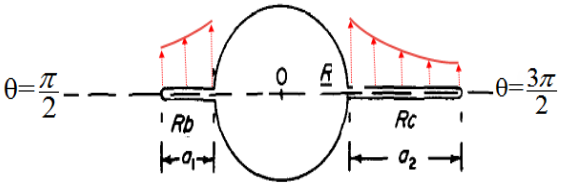

Figure 8. Stress entrance to the crack

Now we consider that a crack is emanated from the hole. When the circular hole with crack is acted on by stress wave, the front of wave is diffracted by the boundary of hole. Then the concentrated stress around the hole acted on the crack. The mathematical relation of this stress is calculated in the equation 5 via time and distance from circular hole.

$$\sigma_{\theta\theta}(x)=-0.85\frac{x^4}{R^4}+4.16\frac{x^3}{R^3}-5.15\frac{x^2}{R^2}-2.68\frac{x}{R}+7.8 \qquad (5)$$

In [13], the dynamic stress intensity factor in the crack under impact load were calculated. But in this research, it's considered that the stress distribution is uniform and the distribution of stress via position is constant. In the other word, the changes of the stress via x are constant.

Based on the method that used in ref [13] and [14], the coordinate system in Figure 9 is chosen for analyzing the dynamic stress intensity factor.

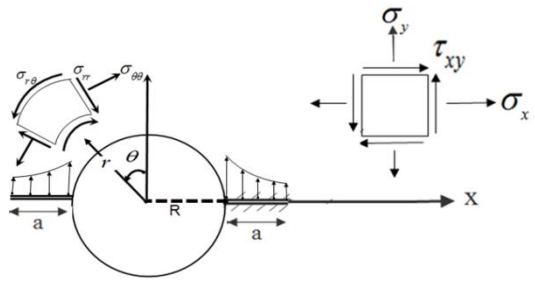

Figure 9. Reference coordinate for crack analysis

The Basic Equation And Solution

Boundary conditions in y=0 is as relation 6[13]:

$$\tau_{xy}(x,0,t)=0, \quad |x|<\infty$$

$$\sigma_y(x,0,t)=\begin{cases}\sigma_0\left[-0.85\frac{x^4}{R^4}+4.16\frac{x^3}{R^3}-5.15\frac{x^2}{R^2}-2.68\frac{x}{R}+7.8\right] \\ +\sigma_0\left[-0.85\frac{x^4}{R^4}+4.16\frac{x^3}{R^3}-5.15\frac{x^2}{R^2}-2.68\frac{x}{R}+7.8\right]_{R<x<R+c|} \\ \left[-0.0023\left(\frac{C_p t}{R}\right)^5+0.0432\left(\frac{C_p t}{R}\right)^4-0.2833\left(\frac{C_p t}{R}\right)^3+\right. \\ \left.0.6885\left(\frac{C_p t}{R}\right)^2-0.0732\left(\frac{C_p t}{R}\right)+0.6455\right]H\left(t+0.5\left(\frac{C_p}{R}\right)\right) \\ R+bR<x<R+cR\end{cases} \quad (6)$$

$$v(x,0,t)=0, \quad |x|>0$$

Where

$$H(t)=\begin{cases}0 & t<0\\ 1 & t>0\end{cases}$$

To solve the stress fields around the crack, two displacements functions of $u(x,y,t)$ and $v(x,y,t)$ are assumed, which both are true in the wave equation[11].

Therefore:

$$\frac{\partial^2 u(x,y,t)}{\partial x^2}+\frac{\partial^2 u(x,y,t)}{\partial y^2}=\frac{1}{C_p^2}\frac{\partial^2 u(x,y,t)}{\partial t^2}$$
$$\frac{\partial^2 v(x,y,t)}{\partial x^2}+\frac{\partial^2 v(x,y,t)}{\partial y^2}=\frac{1}{C_p^2}\frac{\partial^2 v(x,y,t)}{\partial t^2} \quad (7)$$

In these equations, C_p is longitudinal wave speed, C_s is shear wave speed, u is displacement at x, and v is displacement in y direction.

The relationship between stress and displacement fields is defined as follows:

$$\tau_{ij}=\lambda u_{k,k}\delta_{ij}+\mu(u_{i,j}+u_{j,i}) \quad (8)$$

Where:

$$\lambda=\frac{\nu E}{(1+\nu)(1-2\nu)} \qquad \mu=\frac{E}{2(1+\nu)}$$

$$C_p=\left(\frac{\lambda+2\mu}{\rho}\right)^{\frac{1}{2}} \qquad C_s=\left(\frac{\mu}{\rho}\right)^{\frac{1}{2}}$$

Consequently:

$$\sigma_{yy}=(2\mu+\lambda)\frac{\partial v}{\partial y}+\lambda\left(\frac{\partial u}{\partial x}\right)$$
$$\tau_{xy}=\mu\left(\frac{\partial u}{\partial y}+\frac{\partial v}{\partial x}\right) \quad (9)$$

As the analytical solution is difficult in a time-place environment, to solve them, they are first taken to Laplace environment. Then, With respect to the geometrical symmetry, the Fourier sine and cosine transform is used for solving the problems.

To do so, Laplace transform is defined as follows:

$$\bar{f}(s)=\int_0^\infty f(t)e^{-st}dt \qquad f(t)=\frac{1}{2\pi i}\int_{Br}\bar{f}(s)e^{st}dt \quad (10)$$

Now, Laplace is taken of equation 7 versus time consequently:

$$\frac{\partial^2 \bar{u}(x,y,s)}{\partial x^2}+\frac{\partial^2 \bar{u}(x,y,s)}{\partial y^2}=\frac{s^2}{C_p^2}\bar{u}(x,y,s)$$
$$\frac{\partial^2 \bar{v}(x,y,s)}{\partial x^2}+\frac{\partial^2 \bar{v}(x,y,s)}{\partial y^2}=\frac{s^2}{C_p^2}\bar{v}(x,y,s) \quad (11)$$

Now, the Fourier sine and cosine transform, which is defined as relation 12 and 13, are used for transforming relation 11 into an ordinary differential equation.

$$F(p)=\int_0^\infty f(x)\sin(px)dx \qquad f(x)=\frac{2}{\pi}\int_0^\infty F(p)\sin(px)dp \quad (12)$$

$$F(p)=\int_0^\infty f(x)\cos(px)dx \qquad f(x)=\frac{2}{\pi}\int_0^\infty F(p)\cos(px)dp \quad (13)$$

By applying the transforms of relation 12 and 13 in equation 11, we have

$$-p^2U(p,y,s)+\frac{\partial^2 U(p,y,s)}{\partial y^2}=\frac{s^2}{C_p^2}U(p,y,s)$$
$$-p^2V(p,y,s)+\frac{\partial^2 V(p,y,s)}{\partial y^2}=\frac{s^2}{C_p^2}V(p,y,s) \quad (14)$$

Which are two ordinary differential equations and their general solution is as relation 15:

$$U(p,y,s)=A(p,s)e^{-\gamma_1 y}+A_1(p,s)e^{\gamma_1 y}$$
$$V(p,y,s)=B(p,s)e^{-\gamma_1 y}+B_1(p,s)e^{\gamma_1 y} \quad (15)$$

Where $\gamma_1=\left(p^2+\frac{s^2}{C_p^2}\right)^{\frac{1}{2}}$ and $\gamma_1=\left(p^2+\frac{s^2}{C_s^2}\right)^{\frac{1}{2}}$ and $A_1(p,s)$ and $B_1(p,s)$ are vanished because when y tends to infinity, displacement value cannot be infinite. By taking reverse integration of equation15, we have:

$$\bar{u}(x,y,s)=\int_0^\infty A(p,s)e^{-\gamma_1 y}\sin(px)dp \tag{16}$$

$$\bar{v}(x,y,s)=\int_0^\infty B(p,s)e^{-\gamma_1 y}\cos(px)dp \tag{17}$$

Now, we have two equations based on x, y and p. To impose boundary conditions, first, Laplace transform is applied to them. Therefore:

$$\bar{\sigma}_{yy}(x,y,s)=(2\mu+\lambda)\frac{\partial\bar{v}}{\partial y}+\lambda\left(\frac{\partial\bar{u}}{\partial x}\right) \tag{18}$$

$$\bar{\tau}_{xy}(x,y,s)=\mu\left(\frac{\partial\bar{u}}{\partial y}+\frac{\partial\bar{v}}{\partial x}\right) \tag{19}$$

$$\bar{\tau}_{xy}(x,0,s)=0,\quad |x|<\infty \tag{20}$$

$$\sigma_y(x,0,t)=\left\{\sigma_0\left[-0.85\frac{x^4}{R^4}+4.16\frac{x^3}{R^3}-5.15\frac{x^2}{R^2}-2.68\frac{x}{R}+\right.\right.$$
$$+\sigma_0\left[-0.85\frac{x^4}{R^4}+4.16\frac{x^3}{R^3}-5.15\frac{x^2}{R^2}-2.68\frac{x}{R}+7.8\right]_{R<x<R}$$
$$\times\frac{1}{s^6}\left[-0.28\left(\frac{C_p}{R}\right)+1.04\left(\frac{C_p}{R}\right)^4 s+1.7\left(\frac{C_p}{R}\right)^3 s^2+1.3\right. \tag{21}$$
$$\left.\left.+0.07\left(\frac{C_p}{R}\right)s^4+0.65s^5\right]\right. \quad R+bR<x<R+cR$$

$$\bar{v}(x,0,s)=0,\ |x|>0 \tag{22}$$

By replacing equations 16 and 17 in equation 19 and applying boundary conditions 20, 21 and 22 and inserting y=0, we have:

$$\bar{\tau}_{xy}\Big|_{y=0}=\int_0^\infty\left[\gamma_1 A(p,s)-pB(p,s)\right]\sin(px)dp=0$$
$$\text{Þ}B(p,s)=D(p,s)\quad\text{and}\quad A(p,s)=\frac{p}{\gamma_1}D(p,s) \tag{23}$$

by replacing 16 and 17 in equation 18 and applying boundary conditions 20, 21 and 22 and inserting y=0:

$$\bar{\sigma}_y\Big|_{y=0}=\int_0^\infty pF(p,s)D(p,s)\cos(px)dp=$$
$$\left\{\sigma_0\left[-0.85\frac{x^4}{R^4}+4.16\frac{x^3}{R^3}-5.15\frac{x^2}{R^2}-2.68\frac{x}{R}+7.8\right]_{R+bR<x<R}\right.$$
$$\left.+\sigma_0\left[-0.85\frac{x^4}{R^4}+4.16\frac{x^3}{R^3}-5.15\frac{x^2}{R^2}-2.68\frac{x}{R}+7.8\right]_{R<x<R+cR}\right\}$$
$$\times\frac{1}{s^6}\left[-0.28\left(\frac{C_p}{R}\right)+1.04\left(\frac{C_p}{R}\right)^4 s+\right. \tag{24}$$
$$\left.1.7\left(\frac{C_p}{R}\right)^3 s^2+1.38\left(\frac{C_p}{R}\right)^2 s^3\right]$$
$$\text{where } F(p,s)=\left[(2\mu+\lambda)\frac{\gamma_2}{p}+\lambda\frac{p}{\gamma_1}\right]$$

Meanwhile, with respect to the boundary condition 22, we have

$$\bar{v}\Big|_{y=0}=\int_0^\infty D(p,s)\cos(px)dp=0 \tag{25}$$

As a result, a dual integral equation is obtained, which is defined as follows:

$$\int_0^\infty pF(p,s)D(p,s)\cos(px)dp=$$
$$\left\{\sigma_0\left[-0.85\frac{x^4}{R^4}+4.16\frac{x^3}{R^3}-5.15\frac{x^2}{R^2}-2.68\frac{x}{R}+7.8\right]_{R+bR<x<R}\right.$$
$$\left.+\sigma_0\left[-0.85\frac{x^4}{R^4}+4.16\frac{x^3}{R^3}-5.15\frac{x^2}{R^2}-2.68\frac{x}{R}+7.8\right]_{R<x<R+cR}\right\} \tag{26}$$
$$\times\frac{1}{s^6}\left[-0.28\left(\frac{C_p}{R}\right)+1.04\left(\frac{C_p}{R}\right)^4 s\right.$$
$$\left.+1.7\left(\frac{C_p}{R}\right)^3 s^2+1.38\left(\frac{C_p}{R}\right)^2 s^3\right]$$

$$\int_0^\infty D(p,s)\cos(px)dp=0 \tag{27}$$

To solve the above dual integral equation, we assume that[13]:

$$D(p,s)=\int_0^a \varphi(\tau,s)J_0(p\tau)d\tau \tag{28}$$

Also, using of two properties of Integral equation that shows in relations 29 and 30 [16].

$$f(x)=\int_a^x \frac{g(\tau)d\tau}{(x^2-\tau^2)^{\zeta}}, \qquad 0<\zeta<1$$
$$g(x)=\frac{2\sin(\pi\zeta)}{\pi}\frac{d}{dx}\int_a^x \frac{\tau f(\tau)d\tau}{(x^2-\tau^2)^{1-\zeta}} \tag{29}$$

$$\int_0^{\infty} \cos(px)J_0(p\tau)d\tau=\begin{cases}\frac{1}{\sqrt{t^2-x^2}}, & x<\tau\\ 0, & x>\tau\end{cases} \tag{30}$$

By replacing equation 28 in relation 26 and using relations 29 and 30, we have:

$$\varphi(\tau,s)+\int_0^a \varphi(\theta,s)K(\theta,s)d\theta=$$
$$-\tau\left\{\sigma_0\left[-0.85\frac{x^4}{R^4}+4.16\frac{x^3}{R^3}-5.15\frac{x^2}{R^2}-2.68\frac{x}{R}+7.8\right]_{R+bR<x<R}\right.$$
$$\left.+\sigma_0\left[-0.85\frac{x^4}{R^4}+4.16\frac{x^3}{R^3}-5.15\frac{x^2}{R^2}-2.68\frac{x}{R}+7.8\right]_{R<x<R+cR}\right\}$$
$$\times\frac{1}{s^6}\left[-0.28\left(\frac{C_p}{R}\right)+1.04\left(\frac{C_p}{R}\right)^4 s\right.$$
$$\left.+1.7\left(\frac{C_p}{R}\right)^3 s^2+1.38\left(\frac{C_p}{R}\right)^2 s^3\right]$$
$$K(\theta,s)=\tau\int_0^{\infty} p(F(p,s)-1)J_0(p\tau)J_0(p\theta)dp$$

To solve the above equation, $\varphi(\theta,s)$ value should be calculated. By putting this value in relation 31 and calculating $\varphi(\tau,s)$ and finally replacing it in 28 and the result in equation 24, $\bar{\sigma}_y$ value is obtained.

Meanwhile, for r=x-R-a,r<<a , dynamic stress intensity factor in a Laplace environment and $\bar{\sigma}_y$ stress value are as relation 32[30]:

$$\bar{\sigma}_y=\frac{\bar{K}_1(s)}{\sqrt{2\pi r}} \tag{32}$$

Where, r is the point very close to crack tip.
Therefore

$$\bar{K}_1=\frac{f(a)}{\sqrt{a}} \tag{33}$$

To solve equation 31, first, the relation is non-dimensional by changing the following variables.

$$\tau=ar, \qquad \theta=a\rho, \qquad \delta=ap \tag{34}$$

As a result:

$$f(t)=f(ar)=-\sigma_0 a^{\frac{1}{2}}\Phi(r)$$
$$\times\left\{\sigma_0\left[-0.85\frac{x^4}{R^4}+4.16\frac{x^3}{R^3}-5.15\frac{x^2}{R^2}-2.68\frac{x}{R}+7.8\right]_{R+bR<x<R}\right.$$
$$\left.+\sigma_0\left[-0.85\frac{x^4}{R^4}+4.16\frac{x^3}{R^3}-5.15\frac{x^2}{R^2}-2.68\frac{x}{R}+7.8\right]_{R<x<R+cR}\right\}$$
$$\times\frac{1}{s^6}\left[-0.28\left(\frac{C_p}{R}\right)+1.04\left(\frac{C_p}{R}\right)^4 s\right. \tag{35}$$
$$\left.+1.7\left(\frac{C_p}{R}\right)^3 s^2+1.38\left(\frac{C_p}{R}\right)^2 s^3\right]$$
$$\Phi(r,s)+\int_0^1 \Phi(\rho,s)L(a\rho,ar)d\rho=r^{\frac{1}{2}}$$
$$L(a\rho,ar)=(r\rho)^{\frac{1}{2}}\int_0^1 \delta\left[F(\delta/a,s)-1\right]J_0(\delta r)J_0(\delta\rho)d\delta$$

After solving the above relation and replacing it in relation 33, we have the equation 36.

The dynamic stress intensity factor in a Laplace environment will be obtained using relation 37

To calculate this factor in a place-time environment, it is necessary to apply the reversed Laplace transform as showed in equation 36.

The numerical method and software MATLAB cod are used for calculating relation 37.

The method used for numerical solution of this relation is mentioned in[31-32]. By calculating $\Phi(1,s)$ and including it in relation 37, the dynamic tension intensity factor is calculated.

$$\bar{K}_1(s)=-\sigma_0 a^{\frac{1}{2}}\Phi(1,s)\times$$
$$\left\{\sigma_0\left[-0.85\frac{x^4}{R^4}+4.16\frac{x^3}{R^3}-5.15\frac{x^2}{R^2}-2.68\frac{x}{R}+7.8\right]_{R+bR<x<R}\right.$$
$$\left.+\sigma_0\left[-0.85\frac{x^4}{R^4}+4.16\frac{x^3}{R^3}-5.15\frac{x^2}{R^2}-2.68\frac{x}{R}+7.8\right]_{R<x<R+cR}\right\} \tag{36}$$
$$\times\frac{1}{s^6}\left[-0.28\left(\frac{C_p}{R}\right)+1.04\left(\frac{C_p}{R}\right)^4 s\right.$$
$$\left.+1.7\left(\frac{C_p}{R}\right)^3 s^2+1.38\left(\frac{C_p}{R}\right)^2 s^3\right]$$

$$K_1(t)=\frac{\sigma_0 a^{\frac{1}{2}}}{2\pi i}\int_{Br}\Phi(1,s)\left\{Q(x)\times\hat{f}(s)\right\}e^{st}ds$$

$$Q(x)=\left[-0.85\frac{x^4}{R^4}+4.16\frac{x^3}{R^3}-5.15\frac{x^2}{R^2}-2.68\frac{x}{R}+7.8\right]_{R+bR<x<R}+$$

$$\sigma_0\left[-0.85\frac{x^4}{R^4}+4.16\frac{x^3}{R^3}-5.15\frac{x^2}{R^2}-2.68\frac{x}{R}+7.8\right]_{R<x<R+cR} \quad (37)$$

$$\hat{f}(s)=\frac{1}{s^6}\left[-0.28\left(\frac{C_p}{R}\right)+1.04\left(\frac{C_p}{R}\right)^4 s+1.7\left(\frac{C_p}{R}\right)^3 s^2+1.38\left(\frac{C_p}{R}\right)^2 s^3\right]$$

DISCUSSION

As mentioned earlier, a large number of cracks are emanated from the hole because of the stress concentration. Knowing the dynamic stress intensity factor for the emanated cracks helps us to predict the probability of crack propagation.

Analytical solution is used to calculate the dynamic stress intensity factor in this study.

The final equation is solved by numerical method in MATLAB code.

To validate the results, firstly, we assume that the amount of R tends to zero and the results are compared with a finite crack under tensile impact pulse in [13].

The results are showed in

Figure **10**.

After validating the accuracy of the obtained equation, we compare the effect of crack length in the equation.

This comparison is done for several different crack sizes via circle radius. The ratios of the crack size to circle radius is considered 0.2, 0.4, 0.6, 0.8, 1, 2.in Figure 12-Figure 16 a comparison is done between dynamic and static stress intensity factor. And also, the results to different ratio of crack size to circular hole radial is shown in Figure 17.

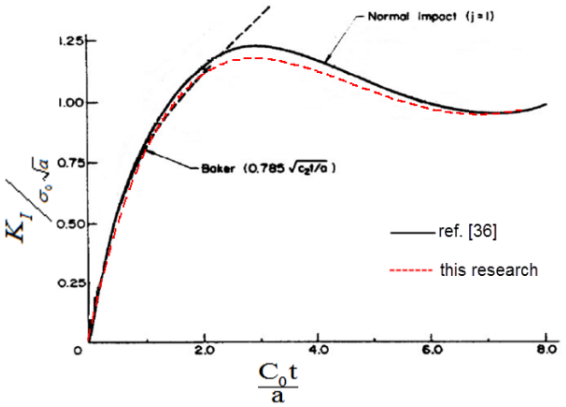

Figure 10. Comparison between last researches and equation 37 result.

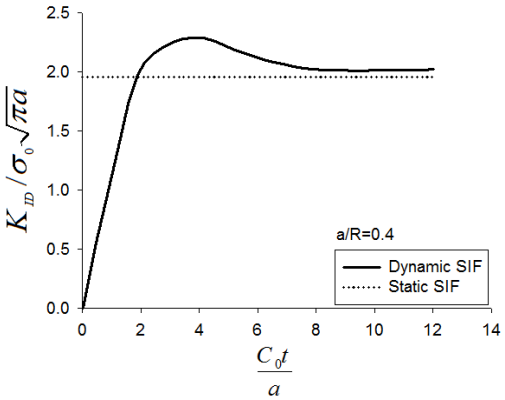

Figure 11. Dynamic stress intensity factor in the a/R=0.2

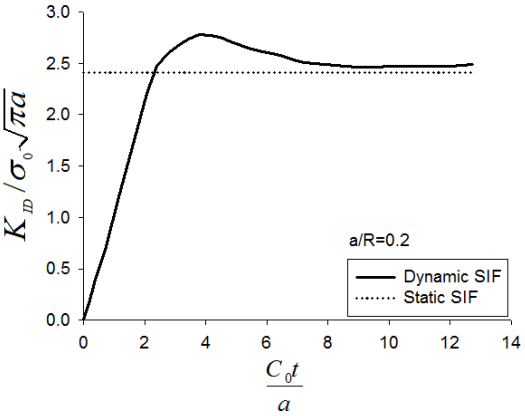

Figure 12. Dynamic stress intensity factor in the a/R=0.4

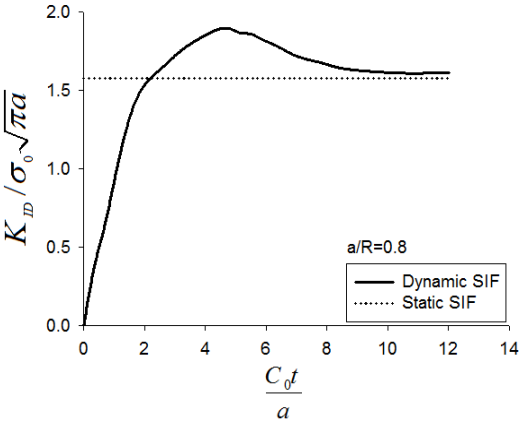

Figure 13. Dynamic stress intensity factor in the a/R=0.6

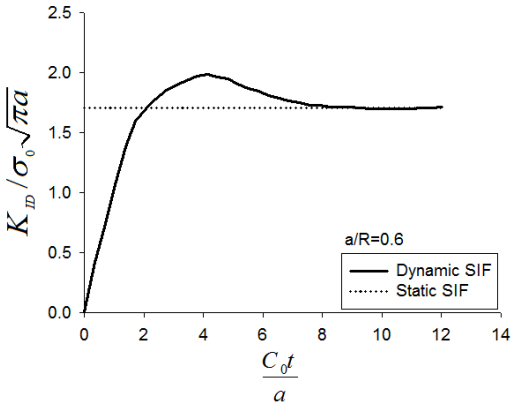

Figure 14. Dynamic stress intensity factor in the a/R=0.8

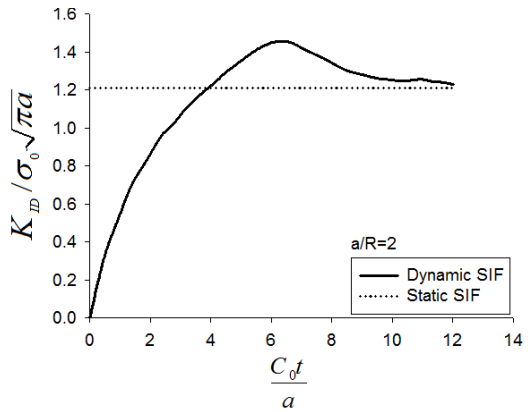

Figure 15. Dynamic stress intensity factor in the a/R=2 and

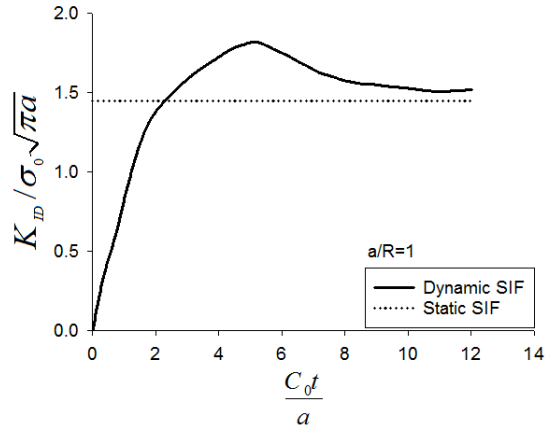

Figure 16. Dynamic stress intensity factor in the a/R=1

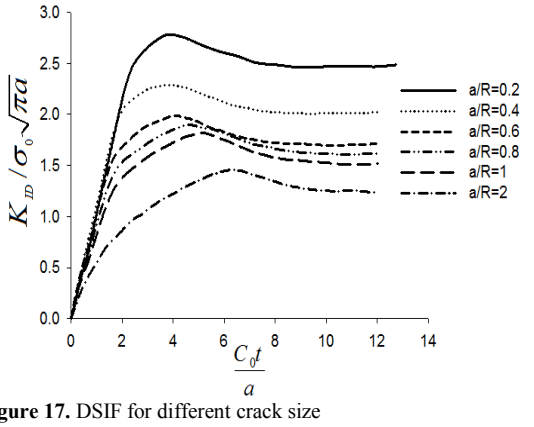

Figure 17. DSIF for different crack size

As we can see in Figure 17, with increasing the crack length, the effect of the stress concentration in the dynamic stress intensity factor is reduced. These changes of the Dynamic stress intensity factor are like static state but the comparison of the peak of the curves with static ratios shows different results. After some time the effect of the inertia reduced and the amount of stress intensity factor tends to the static SIF.

When the crack is not prependicular to the stress wave propagation direction, mode II of the frachture happens. Due to the similartiy of the analytical method for calculating the mode II of fracture under shear stress with normal stress, the results only compared in Figure 18 - Figure 21.

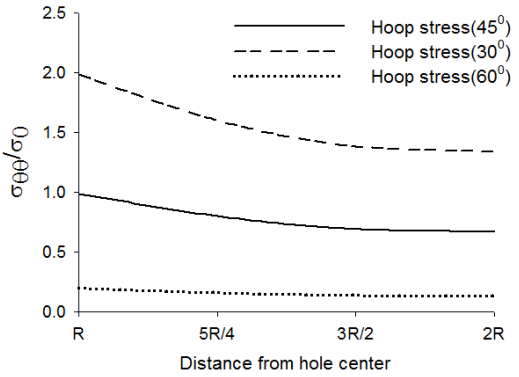

Figure 18. Normal stress distribution around the hole

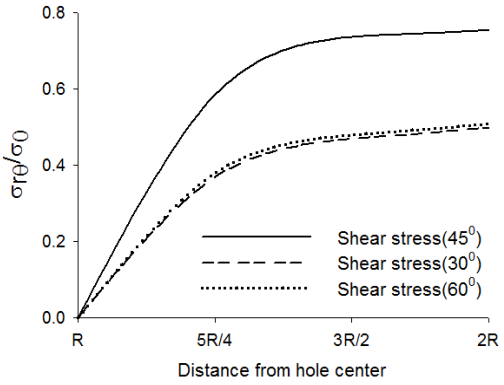

Figure 19. Normal stress distribution around the hole

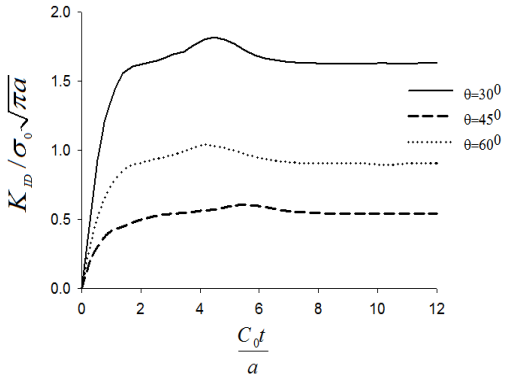

Figure 20. KI in different angles around the hole

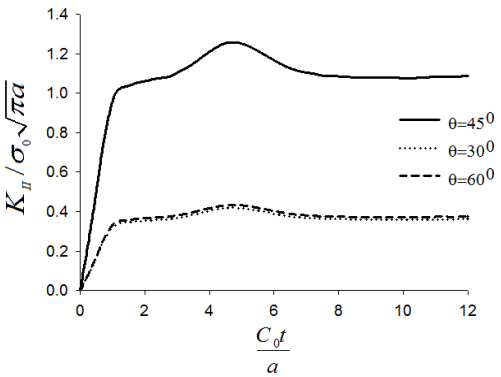

Figure 21. K_{II} in different angles around the hole

As we can see in the figures, the second mode of fracture on in other word, the shear stress in $\theta = 45^{o}$ is maximum.

CONCLUSION

Analytical solution is used to solve the dynamic stress intensity factor for the edge line cracks that emanated from the hole. Firstly, the stress concentration equation around a hole is solved and the stress distribution equations calculated around the hole.

Secondly, by applying the concentrating load equation to the crack plan, the basic equation of stress wave propagation in an elastic medium are derived. These basic equations are solved by Laplace and Fourier transfer to solve the displacements fields and stress distribution around the crack tip to calculate dynamic stress intensity factor.

Finally, the derived equations are solved numerically to calculate the dynamic stress intensity factor for different crack size.

The obtained results show that by decreasing the ratio of the crack length to the circle radius, the dynamic stress intensity factor increases because in small ratios, stress concentration has more effects.

Moreover, it's possible to predict the probability of the crack propagation by the results of this paper for a single edge crack that emanated from a hole.

REFERENCES

[1] Y.-H. Pao, "Dynamical stress concentration in an elastic plate," *Journal of Applied Mechanics,* vol. 29, pp. 299-305, 1962.

[2] M. Baron and A. Matthews, "Diffraction of a pressure wave by a cylindrical cavity in an elastic medium," *Journal of Applied Mechanics,* vol. 28, pp. 347-354, 1961.

[3] M. Baron and R. Parnes, "Displacements and velocities produced by the diffraction of a pressure wave by a cylindrical cavity in an elastic medium," *Journal of Applied Mechanics,* vol. 29, pp. 385-395, 1962.

[4] R. Shea, "Dynamic stress-concentration factors," *Experimental Mechanics,* vol. 4, pp. 20-24, 1964.

[5] A. Haug, *et al.*, "Resonance theory of elastic wave scattering from a cylindrical cavity," *Journal of Sound and Vibration,* vol. 57, pp. 51-58, 1978.

[6] G. Manolis and D. Beskos, "Dynamic stress concentration studies by boundary integrals and Laplace transform," *International Journal for Numerical Methods in Engineering,* vol. 17, pp. 573-599, 1981.

[7] S. Itou, "Diffraction of a stress wave by a cylindrical cavity in an infinite elastic strip," *International journal of engineering science,* vol. 22, pp. 475-490, 1984.

[8] S. Itou, "Diffraction of a stress wave by two circular cylindrical cavities in an infinite elastic strip," *Computers & structures,* vol. 31, pp. 131-137, 1989.

[9] W.-M. Lee and J.-T. Chen, "Scattering of flexural wave in a thin plate with multiple circular holes by using the multipole Trefftz method," *International Journal of Solids and Structures,* vol. 47, pp. 1118-1129, 2010.

[10] K. Shankar, "A study of the dynamic stress concentration factors of a flat plate for SEA applications," *Journal of Sound and Vibration,* vol. 217, pp. 97-111, 1998.

[11] G. C. Sih, *Elastodynamic crack problems* vol. 4: Springer, 1977.

[12] L. B. Freund, *Dynamic fracture mechanics*: Cambridge university press, 1998.

[13] G. Sih, *et al.*, "Impact response of a finite crack in plane extension," *International Journal of Solids and Structures,* vol. 8, pp. 977-993, 1972.

[14] S. A. Thau and L. Tsin-Hwei, "Transient stress intensity factors for a finite crack in an elastic solid caused by a dilatational wave," *International Journal of Solids and Structures,* vol. 7, pp. 731-750, 1971.

[15] L.-q. WANG and B.-z. GAI, "NUMERICAL CALCULATION OF DYNAMIC STRESS INTENSITY FACTORS FOR A SINGLE HOLE-EDGE SLANT CRACK IN A FINITE PLATE," *Engineering Mechanics,* vol. 3, p. 006, 2009.

[16] L.-q. WANG and B.-z. GAI, "Effect of crack face contact on dynamic stress intensity factors for a hole-edge crack," *Journal of Harbin Institute of Technology,* vol. 2, p. 010, 2009.

[17] S. Meguid and X. Wang, "The dynamic interaction of a crack with a circular hole under antiplane loading," *Journal of the Mechanics and Physics of Solids,* vol. 43, pp. 1857-1874, 1995.

[18] L. Dian-kui and C. Zhi-gang, "Scattering of SH-wave by cracks originating at an elliptic hole and dynamic stress intensity factor," *Applied Mathematics and Mechanics,* vol. 25, pp. 1047-1056, 2004.

[19] L. Diankui and L. Hong, "Scattering of sh-waves by an interacting interface linear crack and a circular cavity near bimaterial interface," *Acta Mechanica Sinica,* vol. 20, pp. 317-326, 2004.

[20] J.-F. Lu and A. Hanyga, "Dynamic interaction between multiple cracks and a circular hole swept by SH waves," *International Journal of Solids and Structures,* vol. 41, pp. 6725-6744, 2004.

[21] H. L. Li, *et al.*, "Dynamic Stress Intensity Problem of SH-Wave by Double Linear Cracks near a Circular Hole," *Key Engineering Materials,* vol. 385, pp. 105-108, 2008.

[22] Y.-J. Wang and C.-F. Gao, "The mode III cracks originating from the edge of a circular hole in a piezoelectric solid," *International Journal of Solids and Structures,* vol. 45, pp. 4590-4599, 2008.

[23] J.-H. Guo, *et al.*, "Exact solutions for anti-plane problem of two asymmetrical edge cracks emanating from an elliptical hole in a piezoelectric material," *International Journal of Solids and Structures,* vol. 46, pp. 3799-3809, 2009.

[24] J.-H. Guo and Z.-X. Lu, "Anti-plane analysis of multiple cracks originating from a circular hole in a magnetoelectroelastic solid," *International Journal of Solids and Structures,* vol. 47, pp. 1847-1856, 2010.

[25] T. S. Song, *et al.*, "Dynamic Stress Intensity Factor for a Radial Crack on a Circular Cavity in a Piezoelectric Medium," *Key Engineering Materials,* vol. 452, pp. 273-276, 2011.

[26] M. Malezhik, *et al.*, "Stress wave fields in plates weakened by curvilinear holes with edge cracks," *International Applied Mechanics,* vol. 42, pp. 192-195, 2006.

[27] W. R. Dao, "Solution for an infinite plate with collinear radial cracks emanating from circular holes under biaxial loading by boundary force method," *Engineering fracture mechanics,* vol. 48, pp. 119-126, 1994.

[28] J. Tweed and D. Rooke, "The elastic problem for an infinite solid containing a circular hole with a pair of

radial edge cracks of different lengths," *International journal of engineering science,* vol. 14, pp. 925-933, 1976.

[29] S. Lin, *et al.*, "The solution of cracks emanating from circular holes," *The Journal of Strain Analysis for Engineering Design,* vol. 31, pp. 235-242, 1996.

[30] M. Kassir and K. Bandyopadhyay, "Impact response of a cracked orthotropic medium," *Journal of Applied Mechanics,* vol. 50, pp. 630-636, 1983.

[31] M. K. Miller and J. Guy, WT, "Numerical inversion of the Laplace transform by use of Jacobi polynomials," *SIAM Journal on Numerical Analysis,* vol. 3, pp. 624-635, 1966.

[32] I. N. Sneddon, "Mixed boundary value problems in potential theory," 1966.